Egyptian Journal of Radiology and Nuclear Medicine

RESEARCH

Open Access

Low-dose versus standard-dose normal temporal bone CT in children: a comparison study

R. Rashma[1], Jyoti Kumar[1*], Anju Garg[1], Radhika Batra[1], Ravi Meher[2] and Ankita Phulia[1]

Abstract

Objective To compare the image quality of normal anatomical structures and radiation dose on low-dose (LDCT) and standard-dose (SDCT) temporal bone CT in children.

Methods The study included 45 LDCT (80 kV and 130 mAs) and 45 SDCT (120 kV and 170 mAs) scans in children, 1–15 years of age. LDCT and SDCT scans were analyzed on H60s and H70h reconstruction kernels, respectively. Two readers assessed the image quality for 25 anatomical structures, using a 5-point scale. A score of 3 and above was considered "sufficient" and 2 and below was considered "insufficient" image quality. Image noise, contrast, age and size-specific effective doses were calculated.

Results Despite an increase in image noise on LDCT, image quality remained sufficient for most structures owing to increased image contrast. The median effective dose on LDCT, calculated with age-specific conversion factor, decreased by 72.9% and that calculated with size-specific conversion factor decreased by 81.8% compared to the dose on SDCT.

Conclusion LDCT provides comparable image quality for evaluation of temporal bone with significant reduction in radiation dose in children.

Keywords Computed tomography, Temporal bone, Pediatric, Image noise, Image contrast, Radiation dosimetry

Background

Computed tomography (CT) is a valuable tool in pediatric imaging and delivers more than half of the total collective dose of radiation during diagnostic workup of children for various reasons [1]. It is the first-line imaging modality for temporal bone evaluation with indications like congenital hearing deficit, infection or trauma [2–4]. Although CT is necessary for diagnosis, children need to be protected from ionizing effects of radiation as they are more radio-sensitive, owing to high mitotic rates and longer life expectancy than adults resulting in greater oncogenic effect [5–7]. The lifetime cancer mortality risk is approximately 14% per Sv for a 1-year-old child, 5% per Sv for a middle-aged adult, and < 2% per Sv for a person older than 60 years [8].

The total dose in a CT examination depends on several factors such as scan length, type of scanning (single slice, helical, volume mode), slice thickness, pitch as well as image reconstruction parameters [1]. Various optimization methods can be used to reduce adverse effects of ionizing radiation like scan justification, adequate patient sedation, adjusting technical and scan parameters like decreasing the scan length by focusing on the part to be examined, using thin collimation, low tube current, and voltage based on the age and weight of the patient, avoiding multiphase CT examination, reducing the tube

*Correspondence:
Jyoti Kumar
drjyotikumar@gmail.com
[1] Department of Radiodiagnosis, Lok Nayak Hospital, Maulana Azad Medical College, Jawaharlal Nehru Marg, New Delhi 110002, India
[2] Department of ENT and Head and Neck Surgery, Maulana Azad Medical College, New Delhi, India

Springer Open

© The Author(s) 2024. **Open Access** This article is licensed under a Creative Commons Attribution 4.0 International License, which permits use, sharing, adaptation, distribution and reproduction in any medium or format, as long as you give appropriate credit to the original author(s) and the source, provide a link to the Creative Commons licence, and indicate if changes were made. The images or other third party material in this article are included in the article's Creative Commons licence, unless indicated otherwise in a credit line to the material. If material is not included in the article's Creative Commons licence and your intended use is not permitted by statutory regulation or exceeds the permitted use, you will need to obtain permission directly from the copyright holder. To view a copy of this licence, visit http://creativecommons.org/licenses/by/4.0/.

rotation time and usage of selective organ shielding [4, 5]. There is a direct relationship between the radiation dose and tube current used. Reduction in tube current is the most practical method for reducing the radiation dose in CT. Additionally, the use of lower tube voltage is related to a relative reduction in the production of scattered radiation [9].

The radiation dose in modern helical scanners is measured by the CT dose volume index ($CTDI_{vol}$) and dose length product (DLP). The $CTDI_{vol}$ is the indicator for the mean local radiation dose to the patient within a given scan volume, and it depends on tube voltage (kVp), tube current (mAs), collimation and pitch. The DLP indicates the mean effective dose to the patient of an entire CT examination, estimated by the product of $CTDI_{vol}$ and scan length [5]. These dose indicators allow direct comparison of the estimated radiation dose among the scanners from different vendors.

Despite the heightened radio sensitivity, adult temporal bone CT protocols are often extrapolated to children without applying size-based adapting techniques [10]. However, temporal bone is ideally suited for low-dose CT owing to high intrinsic contrast of the minute anatomical structures being imaged [11]. The study aims to compare the image quality of normal anatomical structures as well as radiation dose on low-dose (LDCT) and standard-dose (SDCT) temporal bone CT in children.

Methods

Subjects

Sixty consecutive pediatric patients from 1 to 15 years of age referred for temporal bone CT with indications like congenital hearing impairment, trauma, infection or external auditory canal atresia were included. The subjects were subdivided into two age groups of 1–7 years and 8–15 years. Low-dose and standard-dose protocols were used alternatively for these patients (30 in each group). Temporal bone CTs showing middle/inner ear dysplasia and fluid/soft tissue/calcific attenuation involving middle/inner ear were excluded from the study. In the low-dose group, five patients had bilateral middle/inner ear abnormalities and two patients had unilateral middle/inner ear abnormalities. These temporal bone CTs were excluded, leaving 48 normal temporal bone scans available for inclusion in the study. Three patients with bilateral middle/inner ear abnormalities and one patient with unilateral middle/inner ear abnormalities were excluded in the standard-dose group, leaving 53 normal temporal bone scans available for inclusion. The first 90 normal temporal bone studies, 45 low-dose and 45 standard-dose were included in the study for final analysis.

Ethical clearance was obtained from the institutional ethics committee (F.1/IEC/MAMC/ (82/10/2020/No 209). For children < 7 years of age, written informed consent was taken from the parent/guardian. For children 7 to 11 years of age, oral assent was taken from the patient in the presence of parent/guardian. Written assent was obtained for children between 12 and 15 years of age.

CT technique

All patients underwent a high-resolution non-contrast CT of the temporal bone on 128 slice multidetector row CT (MDCT) scanner [Seimens SOMATOM Definition AS + CT scanner (Seimens healthcare, Erlangen, Germany)].

Before finalizing the tube voltage and current for LDCT, ten pediatric patients who were planned for temporal bone CT examinations were evaluated using a combination of parameters ranging from 80 to 100 kV and 120 to 140 mAs. These scans were then reviewed by two radiologists with 25 years and 18 years of experience, respectively, in head and neck radiology. Based on the subjective evaluation of quality on these CT examinations, the readers reached the consensus of using 80 kV and 130 mAs for LDCT protocol in the study. These temporal bone scans were not included in the final study set. The parameters used for the SDCT were 120 kV and 170 mAs as followed in our institute. Axial images were obtained for both protocols using collimation-0.6; pitch-0.8; matrix 512 × 512; FOV-80 mm. Temporal bone was imaged from the petrous apex to the inferior tip of mastoid bone. The raw dataset was reconstructed with a section thickness of 0.6 mm using a high-resolution bone algorithm to obtain high-quality axial images separately for each ear. Coronal and sagittal reformatted multiplanar images were generated from these axial images.

Image analysis

Before the analysis of cases included in the study, ten temporal bone CT scans, 5 each acquired on LDCT and SDCT protocols were evaluated by two readers, using two different high-resolution kernels, H60s and H70h available on our equipment. The readers had 25 years and 18 years of experience, respectively, in head and neck radiology. These temporal bone scans were not included in the final study set. The readers reached a consensus of superior subjective scoring on LDCT using H60s kernel and on SDCT with H70h kernel which were finally used for reconstruction. The final study set comprising of 45 low-dose and 45 standard-dose temporal bone CTs was evaluated using appropriate window width/center by each of these two readers independently. Any discrepancy was resolved by consensus.

Qualitative image analysis

A total of 25 anatomical landmarks were categorized into "relatively big structures" and "relatively small structures" based on the perceptive ease of visibility (Table 1). These were evaluated with regard to image quality by using a 5-point rating system designed by Nauer et al. [8].

5- very good delineation of structure and excellent image quality.

4- clear delineation of structure and good image quality.

3- anatomic structures still fully assessable in all parts and acceptable image quality.

2- anatomic structures, but no details assessable, resulting in insufficient image quality.

1- anatomic structures not identifiable due to poor image quality.

The difference between the scores 5 and 4 was less important to the clinical usefulness of a scan than the difference between the scores 3 and 2. Therefore, the image quality scores 5, 4, and 3 were considered "sufficient image quality" and scores 2 and 1 were considered "insufficient image quality."

Quantitative image analysis

The quantitative analysis was done for image noise, signal-to noise ratio, image contrast and radiation dose.

Table 1 Temporal bone anatomical landmarks for image quality assessment

"Relatively big" structures	"Relatively small" structures
Tympanic membrane	Stapes
Malleus	Incudo-stapedial joint
Incus	Stapedius muscle
Incudo-malleolar joint	Round window
Tensor tympani muscle	Oval window
Pyramidal eminence	Spiral osseous lamina
Cochleariform process	Modiolus
Cochlea	Vestibular aqueduct
Vestibule	Cochlear aqueduct
Cochlear aperture	Bony lamella separating the cochlea from fundus of the internal auditory canal
Facial nerve canal segments	Bony lamella at auditory canal fundus
Labryinthine segment	
Tympanic segment	
Mastoid segment	
Internal carotid artery canal	
Jugular foramen	
Mastoid	

Image noise

Image noise for air, bone and soft tissue was quantified as standard deviation of the attenuation value by placing three regions of interests (ROIs) within soft tissue, bone and air [12, 13]. The ROI sizes applied were $30mm^2$, $40mm^2$, $10mm^2$ for soft tissue, bone and air, respectively. The quantified image noise in both the protocols was also compared with the reference value measured by scanning a uniform water phantom.

Signal-to-noise ratio

Signal-to-noise ratio (SNR) was calculated as the mean attenuation value measured using the above ROIs divided by the image noise in the ROI [4].

Image contrast

Image contrast was measured separately for middle and inner ear [2]. The ROI sizes applied for image contrast measurements were 0.5, 0.8, 8 and 2.4 mm^2 for malleus, air (in middle ear), otic capsule and vestibule (in inner ear), respectively.

Image contrast of middle ear was assessed by subtracting the absorption values of the aerated middle ear cavity from that of the malleus head.

$$\text{Contrast}_{\text{middle ear}} = \text{HU}_{\text{malleus}} - \text{HU}_{\text{air}}$$

Image contrast of the inner ear was assessed by subtracting the absorption values of the vestibule from that of the otic capsule.

$$\text{Contrast}_{\text{inner ear}} = \text{HU}_{\text{otic capsule}} - \text{HU}_{\text{vestibule}}$$

Dosimetry

The volumetric CT dose index ($CTDI_{vol}$) and dose length product (DLP) were displayed on the scanner console and stored in a file with the scans. The $CTDI_{vol}$ and DLP for both protocols were compared.

The effective dose was calculated for each scan by two methods.

1. The age-specific effective dose was calculated by multiplying the DLP with a standardized voltage and age-specific conversion factor for head region as per International Commission on Radiological Protection (ICRP) publication 103 recommendation [14] (Table 2).

Table 2 Standardized voltage and age-specific conversion factors for head as per ICRP publication 103 recommendation

Tube voltage (kV)	Age (years)	Conversion factors
80	Newborn	0.0094
	1	0.0056
	5	0.0035
	10	0.0026
	Adult	0.0018
120	Newborn	0.0085
	1	0.0053
	5	0.0035
	10	0.0027
	Adult	0.0019

Effective dose = DLP (mSv) × age-specific conversion factor.

2. The size-specific effective dose was calculated using the size-specific k factor for head which was derived from the effective diameter as given by Romanyukha et al. [15] (Table 3).

Effective diameter was calculated using the formula- $\sqrt{APXTR}$ [15, 16] on an axial image.

where AP-anteroposterior diameter of head.

TR-transverse diameter of head.

These measurements were taken in the center of the scan from skin-to-skin surface.

Table 3 Size-specific k factors for head as given by Romanyukha et al. [15]

Effective diameter (cm)	Size-specific k factor
8	0.010
9	0.009
10	0.009
11	0.008
12	0.007
13	0.007
14	0.006
15	0.005
16	0.004
17	0.002
18	0.002
19	0.001
20	0.001

Effective dose = DLP (mSv) × size-specific conversion factor.

Statistical analysis

Data were analyzed and statistically evaluated using the SPSS-PC-25 version. Qualitative and quantitative data were expressed in median with interquartile range. Depending on normality distribution, a comparison of quantitative data between two groups was tested by the Mann– Whitney U test. A "*p*" value of less than 0.05 was considered statistically significant.

Results

Demographics and image quality assessment

The mean age of pediatric patients was 12.1 years in LDCT and 11.6 years in SDCT, respectively. Eleven (24.4%) temporal bone scans belonged to the age group 1–7 years and 34(75.5%) to the age group 8–15 years, in the LDCT. In the SDCT, 12 (26.6%) temporal bone scans belonged to 1–7 years age group and 33 (73.3%) to 8–15 years age groups.

The median image quality scores for all the "relatively big structures" showed no statistically significant difference between LDCT and SDCT groups except for cochlear aperture, which had a lower median score of 3 on

Table 4 Qualitative image scores for "relatively big structures" using low-dose and standard-dose protocol

Landmarks	Low-dose (n = 45) Median	Standard-dose (n = 45) Median	Mann–Whitney *U* test *p* value
Tympanic membrane	4.0	5.0	0.05
Malleus	5.0	5.0	0.804
Incus	5.0	5.0	0.810
Incudo-malleolar joint	5.0	5.0	0.860
Tensor tympani muscle	3.0	3.0	0.570
Pyramidal eminence	5.0	5.0	0.616
Cochleariform process	3.0	4.0	0.126
Cochlea	5.0	5.0	0.467
Vestibule	5.0	5.0	0.583
Cochlear aperture	3.0	4.0	**0.006**
Facial nerve canal			
Labryinthine segment	5.0	5.0	0.368
Tympanic segment	5.0	5.0	0.595
Mastoid segment	5.0	5.0	0.494
Internal carotid artery canal	5.0	5.0	0.317
Jugular foramen	5.0	5.0	1.000
Mastoid	5.0	5.0	0.317

In our study, p value <0.05 was considered statistically significant, the numbers highlighted in bold indicates, these structures and values had significant difference between LDCT and SDCT

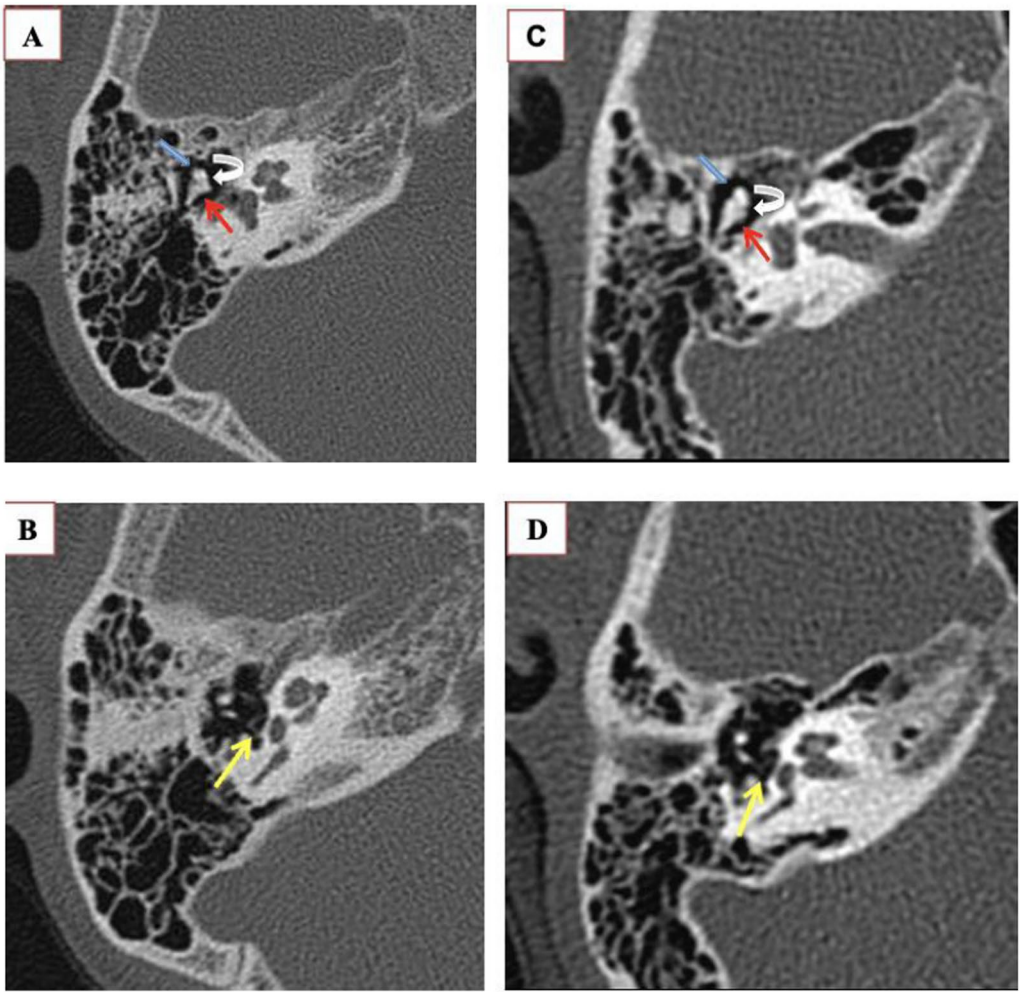

Fig. 1 Image quality assessment of ossicles on axial SDCT **A**, **B** in a 13-year-old girl and axial LDCT **C**, **D** in a 14-year-old girl. The scores given for *malleus* (blue arrow), *the incudo-malleolar joint* (curved arrow) and *incus* (red arrow) were 5 in both SDCT and LDCT protocols; however, *the stapes crus* (yellow arrow) were given a score of 5 in SDCT and 4 in LDCT protocols

low-dose CT scan (Table 4). However, it was still in the "sufficient image quality" range (Figs. 1, 2).

Although the median image quality scores for most of the "relatively small structures" were significantly lower ($p < 0.05$) in the LDCT (Table 5),, these structures showed "sufficient image quality" (Figs. 3, 4, 5). The only exception was the spiral osseous lamina, where the median score fell to 2 with "insufficient image quality" (Fig. 6). The median image quality score for incudo-stapedial joint and round window showed no statistically significant difference between the two groups.

There was no significant difference ($p > 0.05$) in the median image quality scores given for both "relatively big structures" and "relatively small structures" between the age groups 1–7 years and 8–15 years in both LDCT and SDCT protocols.

Quantitative image analysis

Image noise measurements

Image noise measured in the uniform water phantom was 3.8 for fluid, 12 for air on LDCT and 2.5 for fluid and 8 for air on SDCT. The median image noise was 151 for soft tissue, 212 for bone, 109 for air on LDCT and 130 for soft tissue, 189 for bone, 96 for air on SDCT (Figs. 7, 8). Image noise increased in LDCT protocol by 14%, 11% and 12% for soft tissue, bone and air, respectively, compared to SDCT protocol ($p < 0.05$).

Signal-to-noise ratio

The SNR was lower in LDCT protocol compared to SDCT protocol. The median SNR measured for soft tissue, bone, and air were 0.3, 1.6, and -9 for LDCT and 0.4, 1.8, and -7.8 for SDCT protocols as depicted

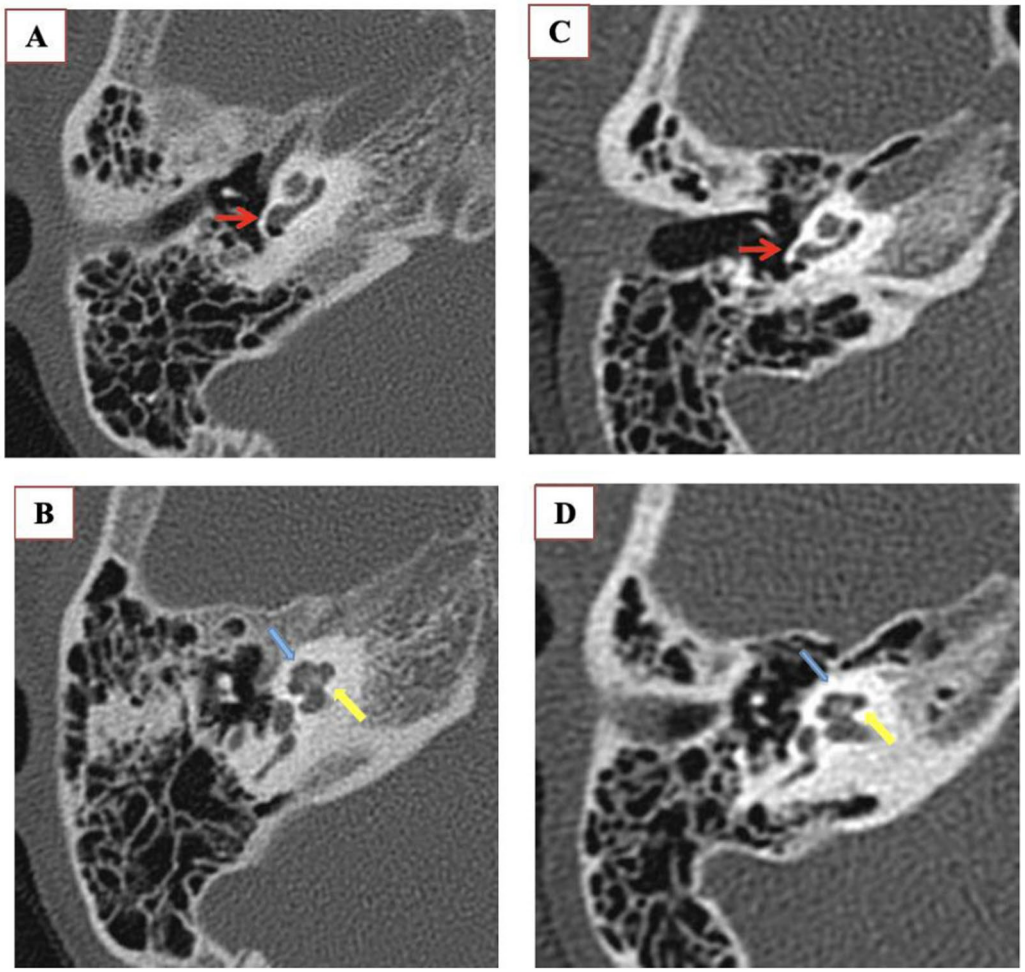

Fig. 2 Image quality assessment of cochlea on axial SDCT **A**, **B** in a 13-year-old girl and axial LDCT **C**, **D** in a 14-year-old girl. The images show basal (red arrow), middle (yellow arrow) and apical turns (blue arrow) of the *cochlea* and the scores given were 5 in both SDCT and LDCT protocol

Table 5 Qualitative image scores for "relatively small structures" using low-dose and standard-dose protocol

Landmarks	Low-dose ($n=45$) Median	Standard-dose ($n=45$) Median	Mann–Whitney *U* test *p* value
Stapes	4.0	5.0	**0.001**
Incudo-stapedial joint	5.0	5.0	0.515
Stapedius muscle	3.0	4.0	**< 0.001**
Round window	5.0	5.0	0.331
Oval window	4.0	5.0	**0.020**
Spiral osseous lamina	2.0	4.0	**< 0.001**
Modiolus	3.0	4.0	**0.006**
Vestibular aqueduct	3.0	4.0	**0.025**
Cochlear aqueduct	3.0	4.0	**0.009**
Bony lamella separating the cochlea from fundus of the internal auditory canal	3.0	4.0	**0.001**
Bony lamella at auditory canal fundus	3.0	4.0	**< 0.001**

In our study, p value <0.05 was considered statistically significant, the numbers highlighted in bold indicates, these structures and values had significant difference between LDCT and SDCT

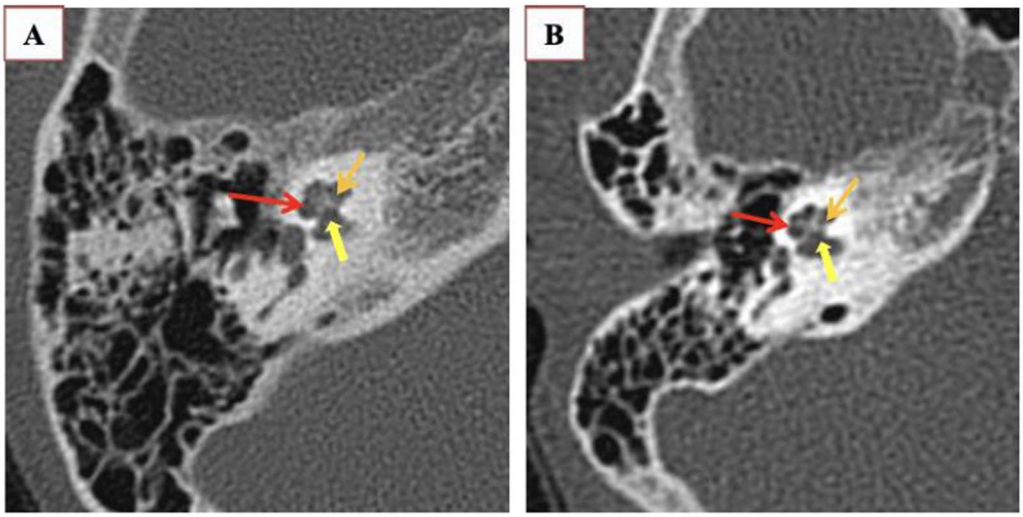

Fig. 3 Image quality assessment of internal cochlear architecture on axial SDCT **A** in a 11-year-old girl and axial LDCT **B** in a 14-year-old girl. *Modiolus* (red arrow) was given a score of 3 in SDCT and 4 in LDCT. *Cochlear aperture* (yellow arrow) was given a score of 5 in both the protocols. *Bony lamella separating the cochlea from fundus of the internal auditory canal (orange arrow)* was given a score of 5 in SDCT protocol and 4 in LDCT protocol

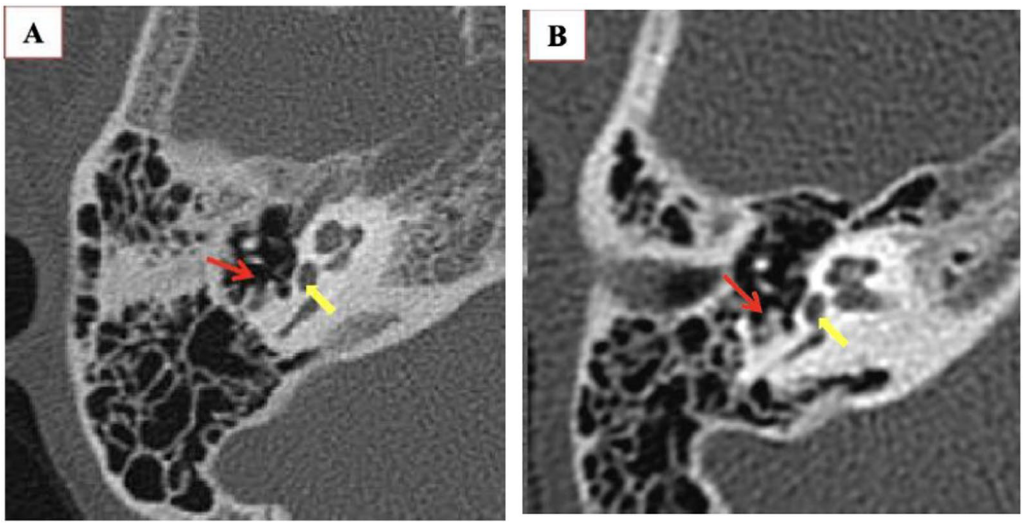

Fig. 4 Image quality assessment of *pyramidal eminence* and *oval window* on axial SDCT **A** in a 4-year-old boy and axial LDCT **B** in a 5-year-old girl. *Both pyramidal eminence* (red arrow) and *oval window* (yellow arrow) were given a score of 5 in SDCT and 4 in LDCT protocols

in Fig. 9. However, the difference was statistically significant only for air ($p < 0.05$).

Image contrast

Image contrast was higher in LDCT group compared to SDCT group. It increased by 27% for middle ear and 25% for inner ear (Figs. 10, 11).

Dosimetry

The $CTDI_{vol}$ and DLP of LDCT scans were approximately 4 times lower than those of SDCT scans. The median effective doses calculated using age and size-specific conversion factors are enumerated in Table 6. The age-specific effective dose decreased by 72.9% and the size-specific effective dose decreased by 81.8% on LDCT as compared to SDCT. All these parameters were statistically significant ($p < 0.05$.)

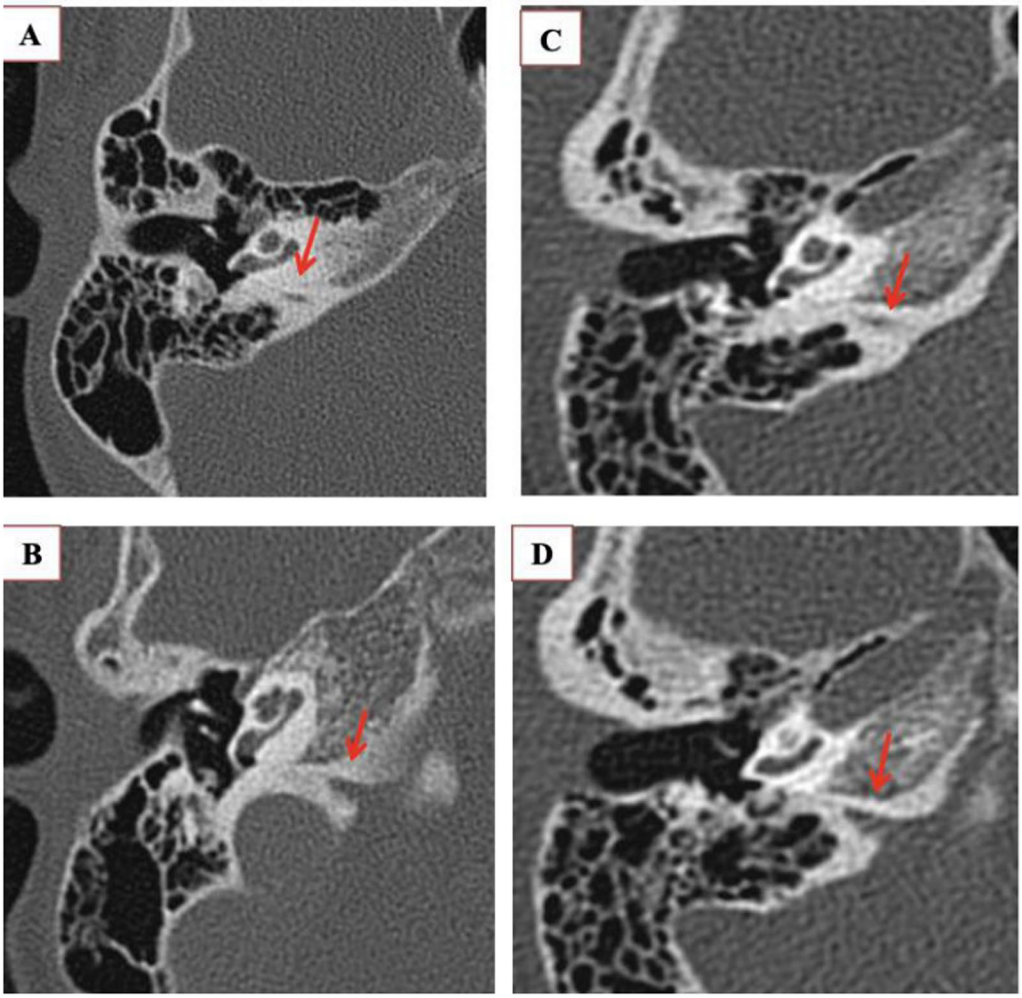

Fig. 5 Image quality assessment of cochlear aqueduct on axial SDCT **A**, **B** in a 13-year-old girl and axial LDCT **C**, **D** in a 14-year-old girl. *Cochlear aqueduct* (red arrow) was given the score of 5 in SDCT and 4 in LDCT protocols

Discussion

The study showed that most of the temporal bone anatomical landmarks in both the categories of "relatively big" and "relatively small" structures had “sufficient image quality” using the LDCT protocol. Among the "relatively big structures" the median image quality score was 5 in both LDCT and SDCT protocols for malleus, incus, incudomalleolar joint, pyramidal eminence, cochlea, vestibule, facial nerve canal segments, internal carotid artery canal, jugular foramen and mastoid. The cochleariform process depicted a median score of 3 in LDCT compared to a median score of 4 in SDCT. However, there was no significant difference ($p > 0.05$) between the two. Cochlear aperture was given the median score of 3 and 4 in LDCT and LDCT protocols, respectively. The low score allotted to the cochleariform process and cochlear aperture in the LDCT protocol was mainly due to the increase in image noise that degraded the image quality. However, the diagnostic image quality level was still maintained for these structures in LDCT scans and mainly the shift of the image quality score was from excellent to good with “sufficient image quality.”

Among the "relatively small structures," there was a statistically significant difference ($p < 0.05$) in the image quality scores between LDCT and SDCT scans for stapes, oval window, modiolus, vestibular aqueduct, cochlear aqueduct, bony lamella separating the cochlea from fundus of the internal auditory canal and bony lamella at auditory canal fundus. "Relatively small structures" which were difficult to visualize on LDCT due to an increase in the image noise still had “sufficient image quality” as the shift of the median score was from excellent to good, within “sufficient image quality” range. The only structure with “insufficient image quality” in LDCT protocol was spiral osseous lamina with a median score of 2 on LDCT and 4 on SDCT ($p < 0.001$). This was likely due to its

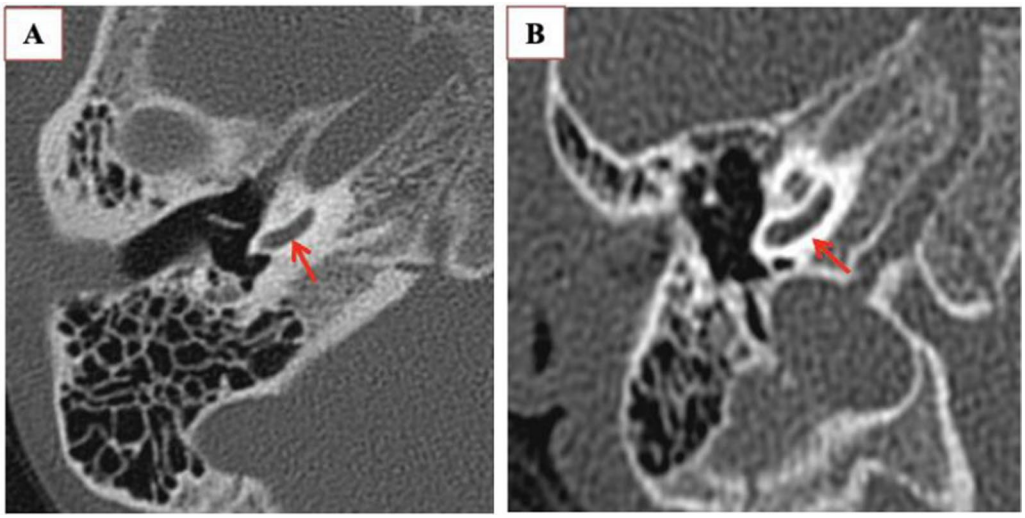

Fig. 6 Image quality assessment of spiral osseous lamina on axial SDCT **A** in a 13-year-old girl and axial LDCT **B** in a 14-year-old girl. The *spiral osseous lamina* (red arrow) was given a score of 4 in SDCT protocol and score of 2 in LDCT protocol

extremely thin anatomy where increased noise in LDCT interfered with its delineation. Tada et al. [17] used LDCT of 120 kV/50mAs and SDCT of 120 kV/100mAs on pediatric temporal bone and found that the image quality was significantly worse for the osseous spiral lamina and posterior crus of the stapes between LDCT and SDCTs. Lutz et al. [9] delineated the temporal bone anatomy using low-dose CT (140mAs and 120 kV) and high-dose CT (180mAs and 120 kV) on adult patients and found significant difference($p < 0.05$) in the image quality between LDCT and SDCT for anterior and posterior crus of the stapes, stapedius muscle, cochlear aqueduct, and tympanic membrane. They found no significant difference in image quality scores in LDCT group for the remaining small anatomical structures. This is in contrast to our study where scores of most of the small anatomical structures were significantly lower on LDCT. This may be due to higher tube voltage of 120 kV used in their low-dose protocol, in contrast to 80 kV used by us. In our study there was no statistically significant difference between LDCT and SDCT protocols ($p > 0.05$) on image quality assessment among different age groups of 1–7 years and 8–15 years.

Image noise was higher in LDCT scans compared to SDCT scans. The median image noise (SD) measured was 151 for soft tissue, 212 for bone, 109 for air on LDCT and 130 for soft tissue, 189 for bone, 96 for air on SDCT. It increased by approximately 14% for soft tissue, 11% for bone, and 12% for air in LDCT protocol as compared to SDCT protocol. The signal-to-noise ratio (SNR) reduced in the LDCT group compared to the SDCT. Although a lower SNR resulted in grainy appearance of the image and reduced image quality that could potentially hamper visualization of various anatomical landmarks, increased image contrast at LDCT protocol resulted in "sufficient image quality." Image contrast increased by 27% for middle ear and 25% for inner ear on LDCT protocol compared with SDCT protocol.

In our LDCT protocol, the median CTDIvol was 5.7 mGy and SDCT protocol was 24.3 mGy. The CTDIvol was approximately 4 times less compared to that of SDCT protocol. The median DLP in our study was 45mGycm for LDCT protocol and 192mGycm for SDCT protocol, it decreased approximately 4–5 times in LDCT with a significant difference ($p < 0.001$) between the two groups.

The median age-specific effective dose was 0.1 mSv for LDCT and 0.37 mSv for SDCT. The dose reduced by 72.9% on LDCT compared to SDCT. The median size-specific effective dose was 0.2 mSv for LDCT and 1.1 mSv for SDCT. The dose reduced by 81.8% on LDCT compared to SDCT. Both the reductions were significant ($p < 0.001$). A study done by Naue et al. [8] on pediatric temporal bone CT found that, in low-dose protocol (80 kV and 90-110 mAs), the effective dose decreased approximately 6 times compared to high-dose protocol (140 kV and 170mAs). The effective doses in our study were lower than those in the above study.

Based on our research findings, we suggest implementing low-dose temporal bone CT protocol of 80 kV and 130 mAs for pediatric patients, which will allow a substantial decrease in the effective dose. In our low-dose protocol, the sole structure exhibiting "insufficient image quality" was spiral osseous lamina, which is a critical

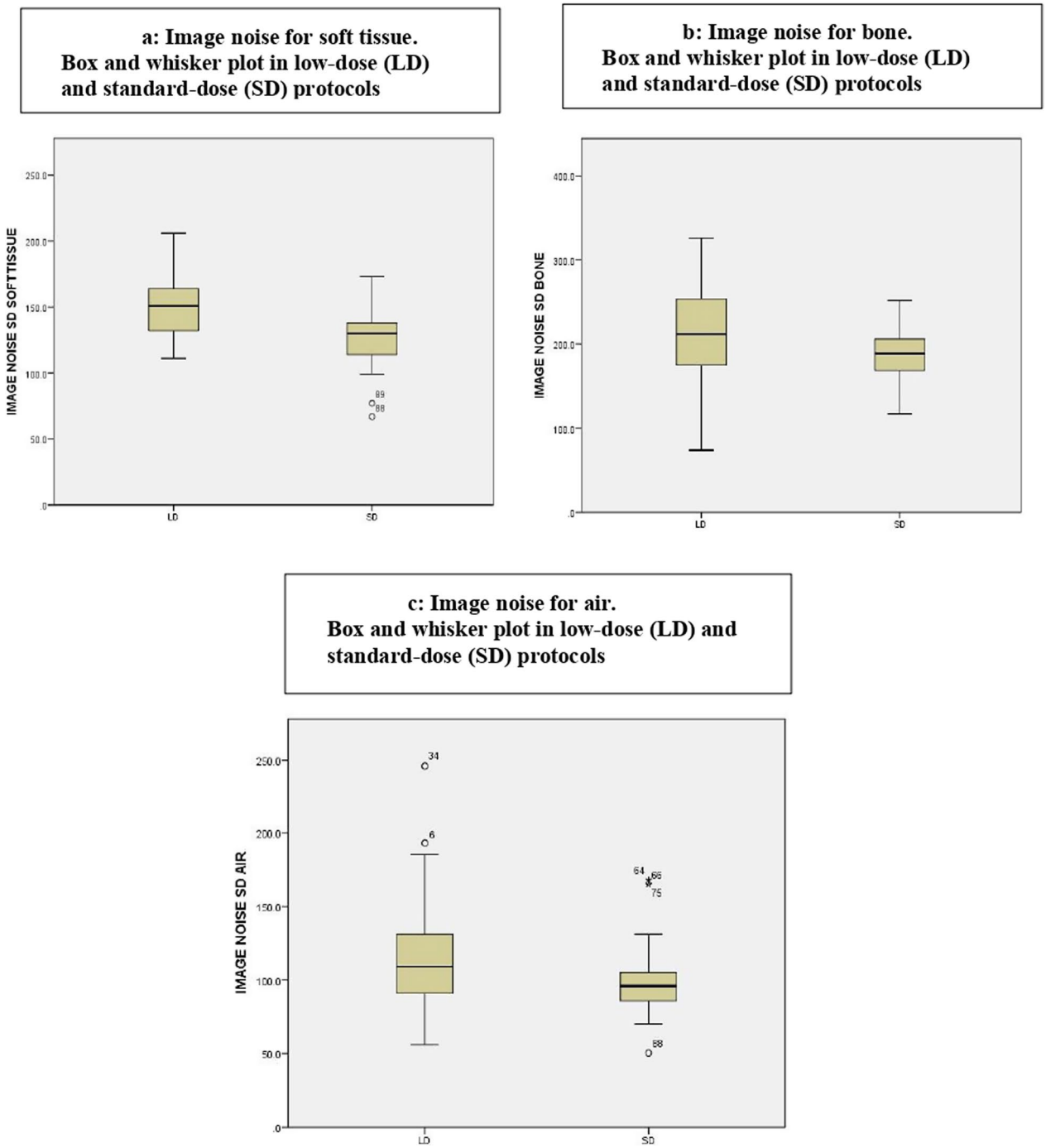

Fig. 7 **a** Image noise for soft tissue. Box and whisker plot in LDCT and SDCT protocols. **b** Image noise for bone. Box and whisker plot in LDCT and SDCT protocols. **c** Image noise for air. Box and whisker plot in LDCT and SDCT protocols

structure in the diagnosis of various inner ear anomalies. Nonetheless, this structure is more effectively visualized on MRI scans. Therefore, LDCT remains a viable option for evaluating temporal bone anatomy in pediatric patients.

Limitations

Our study had several limitations. First, blinding was not feasible during subjective image quality analysis as the reader could recognize both the protocols due to difference in image noise between the two groups. Second,

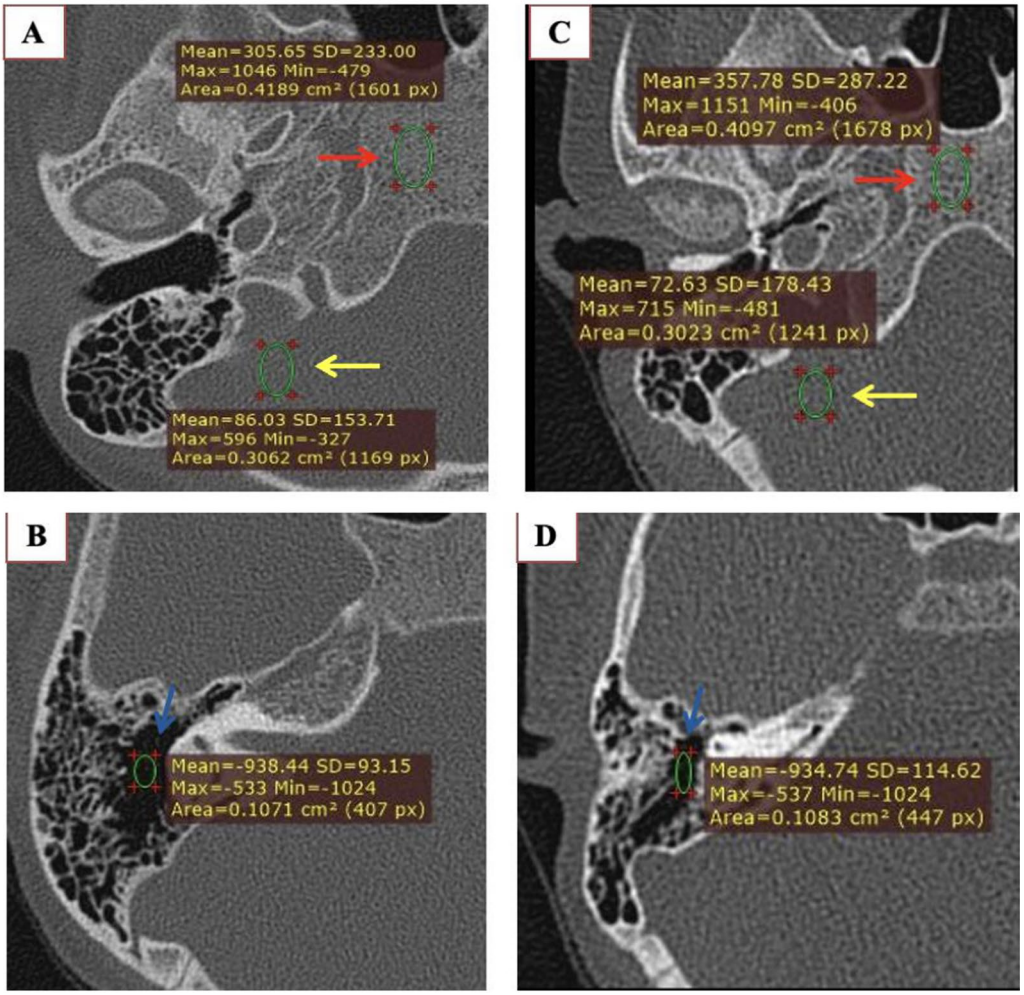

Fig. 8 Image noise assessment on axial SDCT **A**, **B** in a 13-year-old girl and axial LDCT **C**, **D** in a 12-year-old girl. Region of interest measurements was done within soft tissue (yellow arrow), bone (red arrow) and air (blue arrow) for assessing image noise (SD). SDCT: 153 for soft tissue, 233 for bone and 93 for air. LDCT: 178 for soft tissue, 287 for bone and 114 for air. Image noise was higher in low-dose compared to standard-dose CT

only temporal bones with normal anatomy were included in our study and extrapolation to diseased ears needs further validation.

Conclusions

Low-dose temporal bone CT protocol in pediatric population provided a comparable subjective image quality for evaluation of middle and inner ear structures with significant reduction in radiation dose as compared with standard-dose protocol. Though the image quality for few "relatively small structures" reduced significantly, however the diagnostic image quality level was still maintained in low-dose scans and mainly the shift of the image quality score was from excellent to good with "sufficient image quality." In our low-dose protocol, the sole structure exhibiting "insufficient image quality" was spiral osseous lamina, therefore this structure should be evaluated with particular attention on low-dose scans. Despite the raised image noise and fall in signal-to-noise ratio, higher image contrast resulted in a "sufficient" subjective image quality score on the low-dose scan with significantly reduced radiation risk in pediatric population.

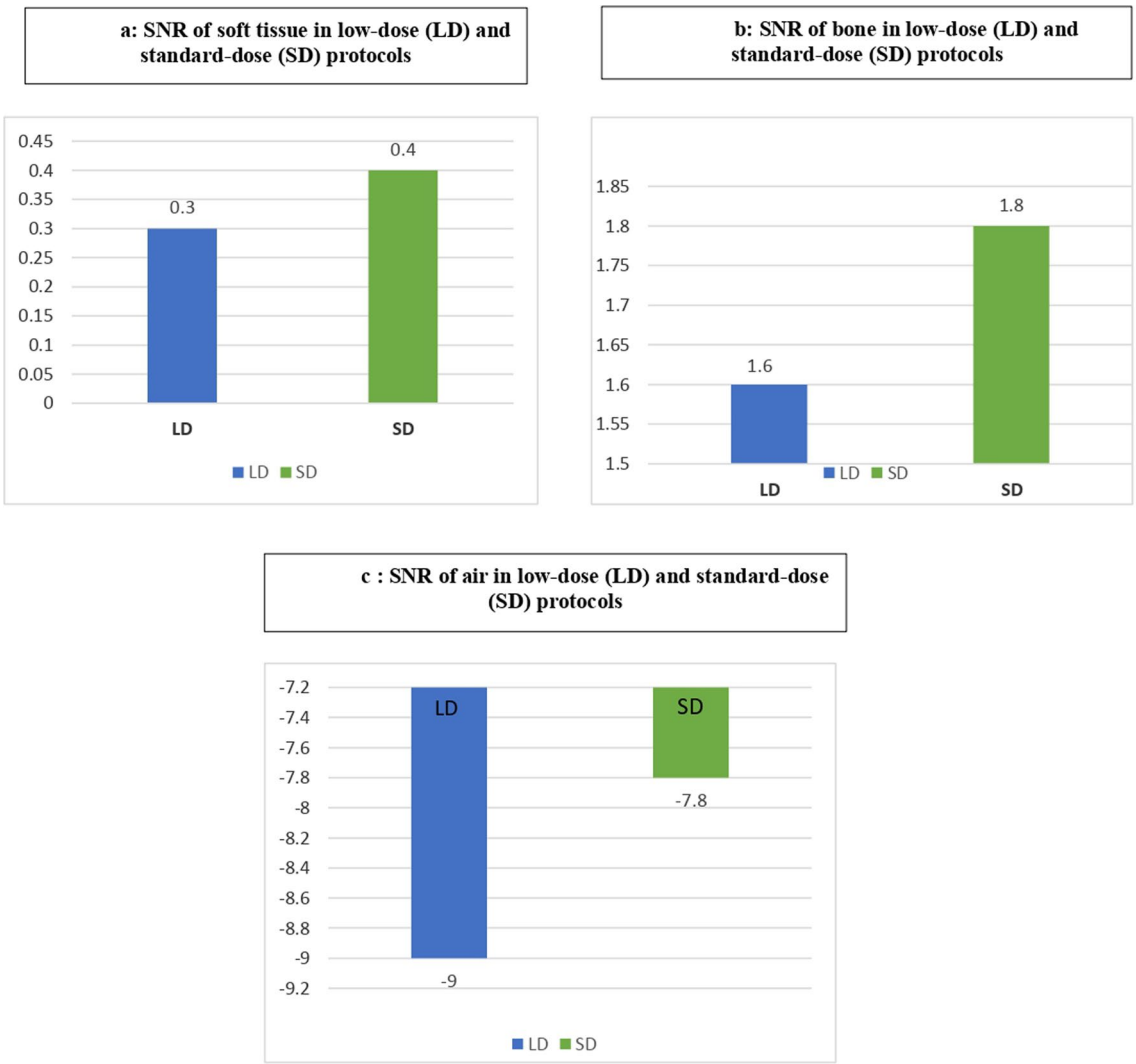

Fig. 9 **a** SNR of soft tissue in LDCT and SDCT protocols. **b** SNR of bone in LDCT and SDCT protocols. **c** SNR of air in LDCT and SDCT protocols

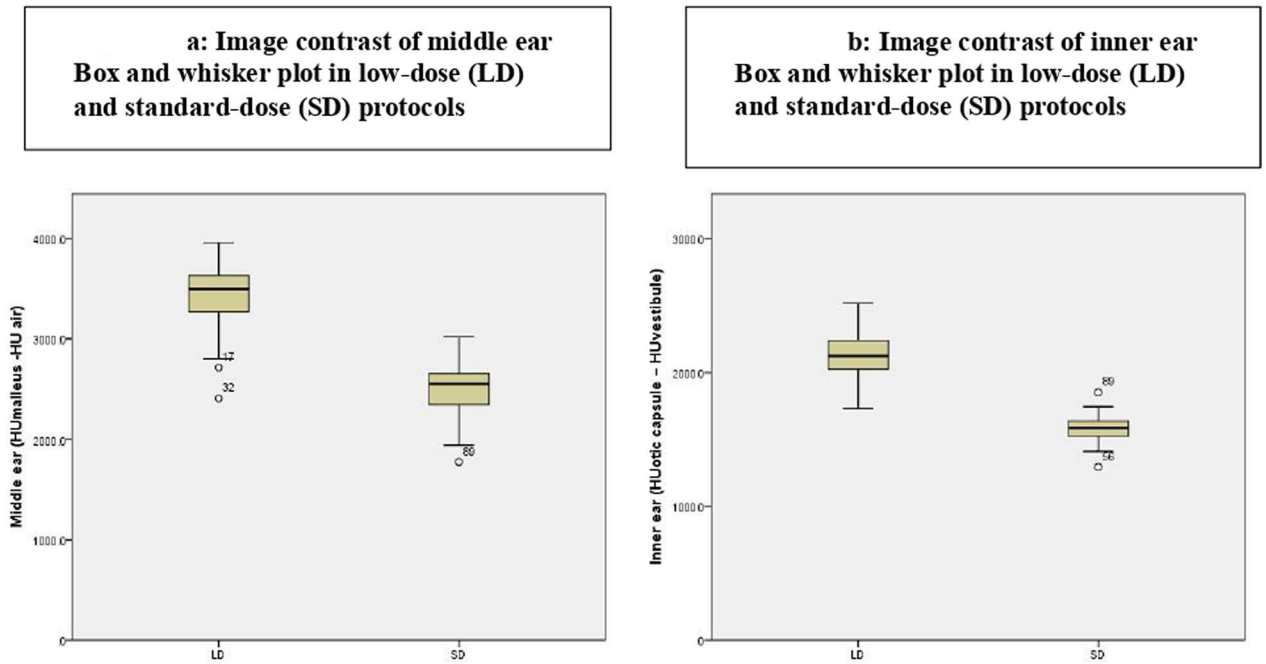

Fig. 10 **a** Image contrast of middle ear. Box and whisker plot in LDCT and SDCT protocols. **b** Image contrast of inner ear. Box and whisker plot in LDCT and SDCT protocols

Table 6 Dosimetry of temporal bone CT on low-dose and standard-dose protocols

Dosimetry	Low-dose ($n=45$) Median	Standard-dose ($n=45$) Median	Mann whitney *U* test *p* value
Volumetric CT dose index (CTDIvol)mGy	5.7	24.3	**< 0.001**
Dose length product (DLP) mGycm	45.0	192.0	**< 0.001**
Age-specific effective dose (mSv)	0.1	0.37	**< 0.001**
Size-specific effective dose (mSv)	0.2	1.1	**< 0.001**

In our study, p value <0.05 was considered statistically significant, the numbers highlighted in bold indicates, these structures and values had significant difference between LDCT and SDCT

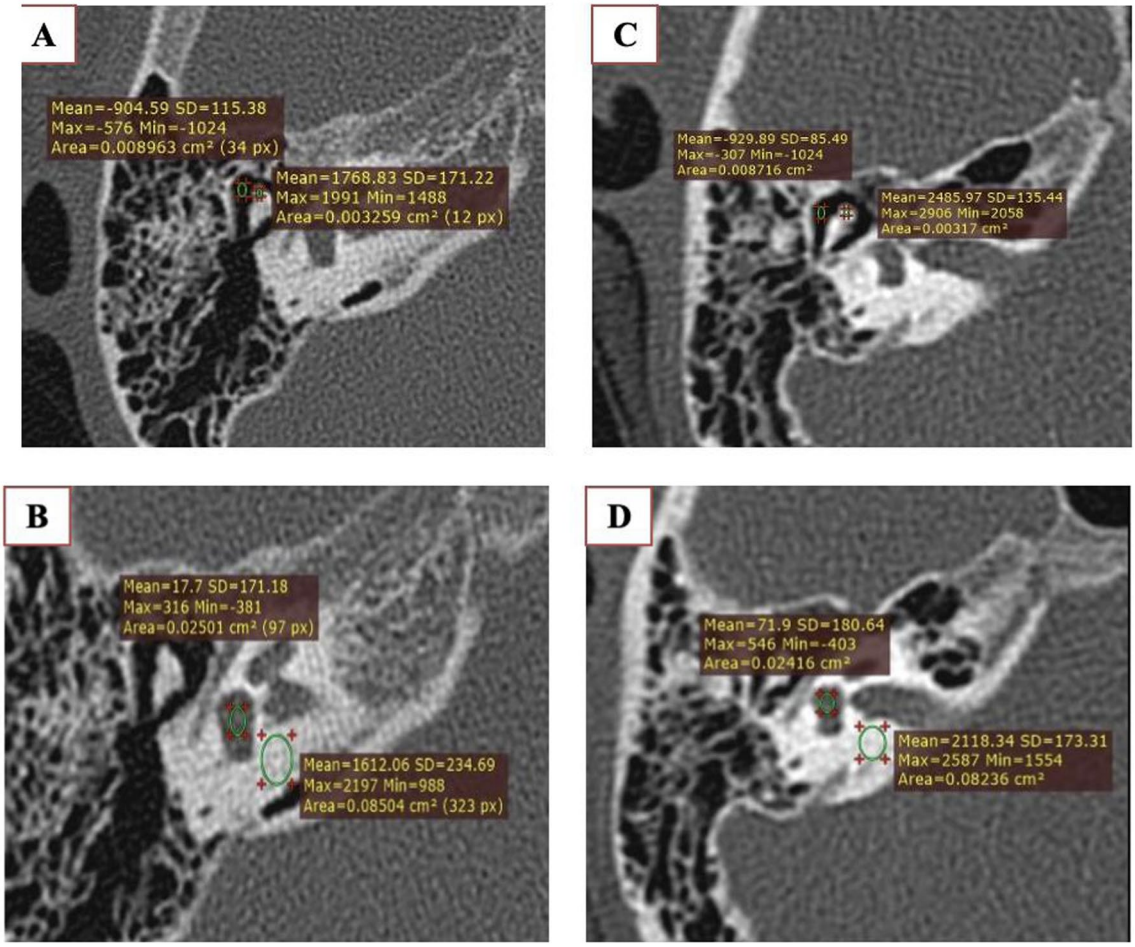

Fig. 11 Image contrast assessment on axial SDCT **A**, **B** in a 13-year-old girl and axial LDCT **C**, **D** in a 12-year-old girl. SDCT:—Middle ear: 1768-(-904) = 2672, inner ear: 1612–17.7 = 1594. LDCT:—Middle *ear*: 2485-(-929) = 3414, inner ear: 2118–71 = 2047. Image contrast was higher in low-dose protocol compared to standard-dose protocol

Abbreviations

CT	Computed tomography
LDCT	Low-dose CT
SDCT	Standard-dose CT
$CTDI_{vol}$	Volumetric CT dose index
DLP	Dose length product
D_{eff}	Effective dose
mSv	Mili Seivert
SNR	Signal-to-noise ratio
MRI	Magnetic resonance imaging

Acknowledgements
None.

Author contributions
R, Kumar and Batra analyzed and interpreted the data and were the major contributors in writing the manuscript. All authors read and approved the final manuscript.

Funding
Not applicable.

Declarations

Ethics approval and consent of participate
Taken.

Consent for publication
Not applicable.

Competing interests
None declared.

Received: 1 January 2024 Accepted: 11 April 2024
Published online: 30 April 2024

References

1. Sorantin E, Weissensteiner S, Hasenburger G, Riccabona M (2013) CT in children–dose protection and general considerations when planning a CT in a child. Euro J Radiol 82:1043–1049
2. Nauer CB, Zubler C, Weisstanner C, Stieger C, Senn P, Arnold A (2011) Radiation dose optimization in pediatric temporal bone computed tomography: influence of tube tension on image contrast and image quality. Neuroradiol 54:247–254

3. Noto D, Funama Y, Kitajima M, Utsunomiya D, Oda S, Yamashita Y (2015) Optimizing radiation dose by varying age at pediatric temporal bone CT. J Appl Clin Med Phys 16:311–318
4. Wang TJ, Wang Y, Zhang ZH, Wang M, Wang M, Su T (2024) Deep learning reconstruction improves the image quality of low-dose temporal bone CT with otitis media and mastoiditis patients. Heliyon 15:10
5. Nievelstein RA, van Dam IM, van der Molen AJ (2010) Multidetector CT in children: current concepts and dose reduction strategies. Pediatr Radiol 40:1324–1344
6. Kofler B, Jenetten L, Runge A, Degenhart G, Fischer N, Hörmann R (2021) ALADA dose optimization in the computed tomography of the temporal bone: the diagnostic potential of different low-dose CT protocols. Diagnostics 11:1894
7. Meulepas JM, Ronckers CM, Smets AM, Nievelstein RA, Gradowska P, Lee C (2019) Radiation exposure from pediatric CT scans and subsequent cancer risk in the Netherlands. JNCI: J Natl Cancer Inst 111:256–263
8. Nauer C, Rieke A, Zubler C, Candreia C, Arnold A, Senn P (2011) Low-dose temporal bone CT in infants and young children: effective dose and image quality. Am J Neuroradiol 32:1375–1380
9. Lutz J, Jäger V, Hempel MJ, Srivastav S, Reiser M, Jäger L (2007) Delineation of temporal bone anatomy: feasibility of low-dose 64-row CT in regard to image quality. Eur Radiol 17:2638–2645
10. Garcia-Carpintero AS, Petcharunpaisan S, Ramalho JP, Castillo M, Mills B (2010) Advances in pediatric orbital magnetic resonance imaging. Expert Rev Ophthalmol 5:483–500
11. Leng S, Diehn FE, Lane JI, Koeller KK, Witte RJ, Carter RE (2015) Temporal bone CT: improved image quality and potential for decreased radiation dose using an ultra-high-resolution scan mode with an iterative reconstruction algorithm. Am J Neuroradiol 36:1599–1603
12. Bauknecht HC, Siebert E, Dannenberg A, Bohner G, Jach C, Diekmann S et al (2010) Image quality and radiation exposure in 320-row temporal bone computed tomography. Dentomaxillofac Radiol 39:199–206
13. Pirimoglu B, Sade R, Sakat MS, Polat G, Kantarci M (2019) Low-dose noncontrast examination of the temporal bone using volumetric 320-row computed tomography. Acta Radiol 60:908–916
14. Deak PD, Smal Y, Kalender WA (2010) Multisection CT protocols: sex- and age-specific conversion factors used to determine effective dose from dose-length product. Radiology 257:158–166
15. Romanyukha A, Folio L, Lamart S, Simon SL, Lee C (2016) Body size-specific effective dose conversion coefficients for CT scans. Radiat Prot Dosimetry 172(4):428–437
16. Kim CR, Jeon JY (2018) Radiation dose and image conspicuity comparison between conventional 120 kVp and 150 kVp with spectral beam shaping for temporal bone CT. Eur J Radiol 102:68–73
17. Tada A, Sato S, Masaoka Y, Kanazawa S (2017) Imaging of the temporal bone in children using low-dose 320-row area detector computed tomography. J Med Imaging Radiat Oncol 61:489–493

Publisher's Note

Springer Nature remains neutral with regard to jurisdictional claims in published maps and institutional affiliations.